J. Fluid Mech. (1986), *vol.* 163, *pp.* 479–497
Printed in Great Britain

The elastohydrodynamic collision of two spheres

By ROBERT H. DAVIS, JEAN-MARC SERAYSSOL
Department of Chemical Engineering, University of Colorado, Boulder, Colorado 80309

AND E. J. HINCH
Department of Applied Mathematics and Theoretical Physics, University of Cambridge

(Received 13 February 1985 and in revised form 19 August 1985)

The dynamic deformation of a solid elastic sphere which is immersed in a viscous fluid and in close motion toward another sphere or a plane solid surface is presented. The deformed shape of the solid surfaces and the pressure profile in the fluid layer separating these surfaces are determined simultaneously via asymptotic and numerical techniques. This research provides the first steps in establishing rational criteria for predicting whether a solid particle will stick or rebound subsequent to impact during filtration or coagulation when viscous forces are important.

1. Introduction

The motion of solid particles in fluids underlies the physics of a host of fascinating phenomena including sedimentation, filtration, coagulation, microbial interactions, slurry transport, and suspension rheology, to name but a few. In many of these applications, a key role is played by collisions or very close relative motion between two interacting particles or between a particle and a solid surface such as the container wall or the surface of a filter fibre. A detailed analysis of this close-contact motion requires consideration of the dynamic shape and separation of the particle surfaces in the vicinity of contact which, in turn, influence the interparticle forces and the hydrodynamic interaction between the particles. On the other hand, the molecular and hydrodynamic forces acting upon the nearly touching surfaces can cause the particles to deform unless they are very rigid. In order to elucidate the basic physics of this near-contact relative motion, this paper considers the dynamic deformation of an elastic sphere which is moving toward a second sphere, or toward a plane surface, under the condition that the two solid objects are separated by a thin fluid layer. The theory takes into account the coupling between the equations of solid mechanics and fluid dynamics that arises naturally in describing collisions of elastic particles in fluids.

A similar coupling between fluid dynamics and elastic solid mechanics is the focus of elastohydrodynamic lubrication theory, which has received considerable attention in the tribology literature. Historically, elastohydrodynamics has been concerned with the deformation of highly loaded gears and bearings as a result of stress distributions in their lubricating fluids. In the current work, we have developed elastohydrodynamic theory for two elastic spheres of arbitrary radii undergoing a collision in a viscous fluid. This problem is of fundamental importance in the areas of filtration, coagulation, and adhesion of small particles.

Recent progress in the areas of the filtration and coagulation of aerosol and

hydrosol dispersions has been summarized by Pruppacher & Klett (1978), Löffler (1980), Prodi & Tampieri (1982), Tien & Payatakes (1979) and Schowalter (1984). Current research continues on related topics such as granular-bed filtration (Gal, Tardos & Pfeffer 1985), dendritic deposition of aerosol particles on filter fibres (Payatakes & Gradon 1980), and the coagulation of sedimenting polydisperse suspensions (Davis 1984; Melik & Fogler 1984). Although these papers vary in the degree of sophistication to which hydrodynamic and colloidal forces are taken into account, their common factor is the use of a trajectory analysis to determine the rate at which collisions occur. Moreover, it is generally assumed that, when a particle collides with another particle or with a filter element, it remains collected. However, as pointed out by several researchers, including Gal *et al.* (1985), Dahneke (1971), and Löffler (1980), the rebounding of particles subsequent to collision may significantly lower the rate of collection. Indeed, for experiments on the collection of micron-sized latex particles in granular-bed and fibre filters, Gal *et al.* (1985), Tsiang, Wang & Tien (1982), Tardos, Pfeffer & Squires (1979), Ellenbecker, Leith & Price (1980), and D'Ottavio & Goren (1983) reported that significant rebounding of particles occurred, as indicated by a decrease in the capture efficiency below theoretical predictions without bouncing. As expected, this particle bouncing increased as the kinetic energy of the particles was increased. No such reduction in the capture efficiency was observed when liquid dioctylphthalate (DOP) aerosols were used. Gal *et al.* (1985) also reported that coating the collector with DOP reduced the bouncing of solid aerosol particles.

The theoretical works mentioned above are very significant in that they provide models for determining the rate at which particle collisions occur. However, in order to obtain a complete understanding of the very important processes of filtration and coagulation, there remains the need for an accurate assessment of the sticking probability (i.e. the fraction of collisions that are not followed by rebound). Intuition and experience tell us that there are two limiting cases. When elastic particles collide in a vacuum, or under conditions of *negligible fluid resistance*, then physical contact occurs. The incoming kinetic energy of the particles is converted into elastic strain energy as they deform in the vicinity of contact. The kinetic energy (other than that dissipated by the internal friction of the solids or remaining as elastic vibrations) is restored as the particles rebound. The sticking probability is essentially zero when the energy dissipated in the solids and fluid is negligible. The theory describing the motion and deformation of elastic particles during such a collision is known as Hertz contact theory and can be found in many textbooks on elasticity (e.g. Love 1927). For the related situation in which the fluid resistance is negligible, but in which a fraction $1-e$ of the incoming kinetic energy is dissipated in the solids, Dahneke (1971, 1972, 1973) and Löffler (1980) have developed a simple model for predicting the critical normal impact velocity which would allow colliding particles to escape (rebound) from an interparticle potential well of a finite depth E. This critical velocity depends upon the coefficient of restitution e and the adhesion energy E, each of whose values are uncertain. Nonetheless, reasonable estimates of these parameters have been made by Dahneke (1973), Tsiang *et al.* (1982), Löffler (1980), and Esmen, Zeigler & Whitfield (1972) in order to get good agreement between theory and experiment. At the opposite extreme, when rigid spheres undergo relative motion in a viscous fluid, the kinetic energy of the spheres is dissipated by non-conservative viscous forces as they approach one another. The rate of close approach is asymptotically slow (Cox & Brenner 1967; Cooley & O'Neill 1969), and the spheres do not deform or rebound.

In between these two limiting cases, it is natural to suppose that a portion of the

incoming kinetic energy of the spherical particles will be dissipated by fluid forces and internal solid friction and that the rest will be transformed into elastic-strain energy of deformation. Depending on the fraction of the kinetic energy that becomes stored as elastic-strain energy, the deformation of the spheres may be significant and rebound may occur. By simultaneously accounting for elastic deformation and viscous fluid forces, the research outlined in this paper provides the first steps in estalishing rational criteria, based on first principles, for determining the range of conditions for which significant deformation and rebound of colliding spheres are predicted when viscous forces are important.

2. Theoretical development

Our theoretical problem follows the motion along the line-of-centres of two elastic spheres. As such, we shall find that the sphere may rebound a small distance after a head-on collision, but that they will not completely separate. A study of oblique collisions will therefore be needed in order to determine the sticking probability. Nonetheless, we expect that the dominant features of the deformation and rebound will result from the component of motion along the line of centres. The two deformable solid surfaces are assumed to be smooth and to be separated by a thin, incompressible Newtonian fluid layer. It is also assumed in this paper that the interparticle forces are negligible and that the fluid layer behaves as a continuum. (See §4 for an elaboration on the effects of interparticle forces and the discrete molecular nature of the fluid on the collision process.) In this case, the thin fluid layer prevents the surfaces from actually touching. However, if the spheres have sufficient inertia as they approach one another, then a large pressure will build up as the fluid is squeezed out from between the spheres. It is this hydrodynamic pressure that causes the elastic solids to deform. The deformed and undeformed surfaces of the two elastic spheres are sketched in figure 1.

For typical solids with large elastic moduli, the relative motion may be divided into inner and outer regions. In the outer region the deformation is negligible as the nearly rigid spheres move from far apart to a position where the separation between their surfaces is small compared to the radius of either sphere. In the inner region the spheres approach even closer together, and the deformation may then become significant. We shall restrict our attention to these final stages of close motion, since it is then that the deformation and rebound that are of interest occur. In our theoretical formulation, we allow the spheres to have arbitrary radii. In the limit, as the radius of one of the spheres goes to infinity, our problem becomes that of a sphere impacting on a plane. For initial conditions, we specify that the spheres start with a distance x_0 between their undeformed surfaces and with a relative velocity v_0 towards one another supplied from the solution for the relative motion in the outer region. We require that x_0 be much smaller than the radius of either sphere and that the spheres be sufficiently rigid so that the surfaces deform only within a small area near the axis of symmetry. (This latter restriction was also made by Muller, Yushchenko & Derjaguin (1983) and by Hughes & White (1979) when studying the static deformation of elastic spheres, and it lies at the heart of the Hertz contact theory of linear elasticity. For most solid particles, this restriction is very reasonable.) The undeformed spherical surfaces can then be approximated by paraboloids in the region of near contact, and the deformed gap profile is given by

$$h(r,t) = x(t) + \frac{r^2}{2a} + w(r,t), \tag{1}$$

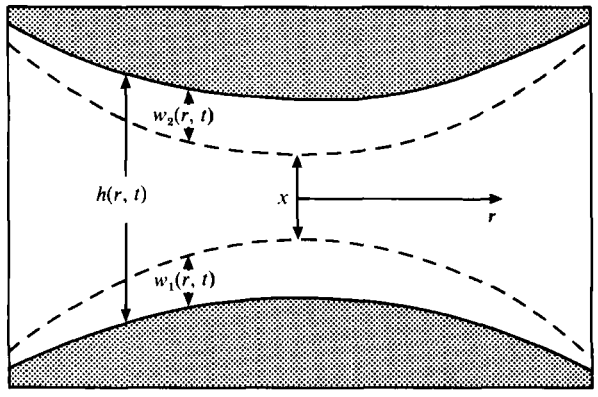

FIGURE 1. Schematic of the deformation of two colliding elastic spheres in a viscous fluid: ——, the actual deformed surfaces; – – –, the undeformed surfaces.

where $x(t)$ is the distance between the undeformed surfaces, $w(r,t) = w_1 + w_2$ is the sum of the dynamic deformations of the two surfaces from their original shape (see figure 1), a is the reduced radius $a_1 a_2/(a_1+a_2)$, and a_i is the radius of sphere i.

In order to determine the deformation $w(r,t)$, we shall follow the development of the Hertz contact theory of linear elasticity (Love 1927) and also the developments of Hughes & White (1979) and Muller *et al.* (1983), who have studied the static deformation of contacting spheres subject to interparticle molecular surface forces. The essence of the theory is that an applied normal force distributed over the surface of an elastic solid will cause it to deform. Provided that this deformation is small, it can be determined by integrating the surface-stress distribution multiplied by a Green function over the area subjected to the stress, where the appropriate Green function is the fundamental solution of the linear-elasticity equations for an applied point force of unit magnitude. For our problem, the formulation of this integral for the surface deformation is (see the Appendix for a derivation):

$$w(r,t) = 4\theta \int_0^\infty f(y,t)\,\phi(r,y)\,\mathrm{d}y, \tag{2}$$

where $f(r,t)$ is the stress distribution over the solid surfaces at the time t. In the present work, we set this equal to the hydrodynamic pressure exerted by the fluid layer; we intend later to include an interparticle potential contribution to the force. The parameter θ is defined as

$$\theta = \frac{1-\nu_1^2}{\pi E_1} + \frac{1-\nu_2^2}{\pi E_2},$$

where ν_i is Poisson's ratio for sphere i, and E_i is Young's modulus of elasticity for sphere i. Also, the Green function kernel $\phi(r,y)$ is given by

$$\phi(r,y) = \frac{y}{y+r} K\left[\frac{4ry}{(r+y)^2}\right], \tag{3}$$

where K is the complete elliptic integral of the first kind (see Abramowitz & Stegun 1964, p. 589–592, for the properties of this elliptic integral). The kernel $\phi(r,y)$ depends only upon the ratio y/r and is plotted in figure 2. A critical feature of (2) is that it is quasi-static, i.e. the deformation is determined only from the instantaneous stress distribution; thus elastic oscillations are neglected. This is justified provided that

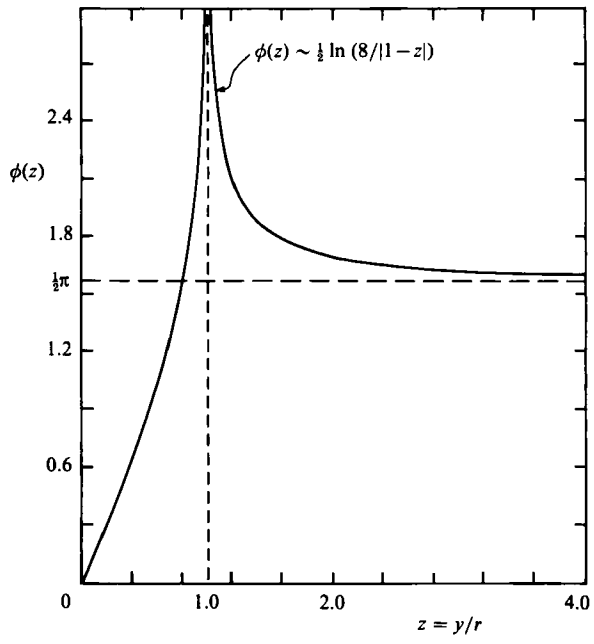

FIGURE 2. The kernel $\phi(y/r)$.

the duration of impact is large compared to the period of vibration. The period of vibration is proportional to a/c, where c is the speed of elastic sound waves in the solid material, whereas the duration of impact τ as given in the absence of fluid by Hertz contact theory is proportional to $a/(c^{\frac{4}{5}}v_0^{\frac{1}{5}})$. The duration of impact can be estimated as follows. The surface displacement of two touching particles travelling at a relative velocity v_0 during time τ is $v_0\tau$. Comparing this to the surface profile (1) gives the radius r of the flattened area to be proportional to $(av_0\tau)^{\frac{1}{2}}$. Hence, an estimate of the elastic strain is $v_0\tau/r$, which gives a total elastic force between the particles on the order of magnitude of $F = \pi r^2 E v_0 \tau/r$. The impulse $F\tau$ must reverse the initial particle momentum $\frac{4}{3}\pi a^3 \rho_s v_0$. Solving the algebra gives the quoted result for τ (noting that $c \approx (E/\rho_s)^{\frac{1}{2}}$, where ρ_s is the solid density and E is Young's elastic modulus). Strictly speaking, the waves can therefore be neglected only when $(v_0/c)^{\frac{1}{5}} \ll 1$, which restricts the analysis to moderate collision velocities (c is on the order of 10^5 cm/s for most solid materials). However, experiments have shown that vibrations can be neglected for nearly all conditions encountered in practice and that a more significant limitation of Hertz contact theory applied to the collisions of spheres is that the resulting deformation should not exceed the elastic limit (Goldsmith 1960; Landau & Lifshitz 1959).

The deformed shape of the sphere surfaces cannot be determined without knowledge of the pressure profile in the fluid layer between the solid surfaces. Since we have restricted our attention to the case where these surfaces are very close to one another, the fluid flow within the narrow gap between them is fully developed to leading order and can be described by the well-known lubrication equation of fluid dynamics (see Hocking 1973 for the method of derivation of this equation):

$$\frac{\partial h}{\partial t} = \frac{1}{12\mu r}\frac{\partial}{\partial r}\left[rh^3\frac{\partial p}{\partial r}\right], \tag{4}$$

where $p(r,t)$ is the pressure profile in the fluid layer which, to leading order, does not vary at any given time across the width of the narrow gap. Also, $h(r,t)$ is defined by (1) and includes the surface deformation; thus (2) and (4) are coupled. In the derivation of (4), the inertia terms are assumed to be small. This is justified provided that $Re\, x_0/a \ll 1$, where the Reynolds number is defined by $Re = \rho v_0 a/\mu$; ρ is the fluid density, and μ is its viscosity. Since x_0/a is assumed to be much less than unity, the inertia of the fluid may be neglected in our analysis even when the Reynolds number is not small. Note, however, that we are assuming in our initial conditions for the deformation $w(r,t)$ that there is negligible elastic deformation in the outer region where fluid inertia can be important.

Finally, in order to complete the formulation of the governing equations, we also require the kinematic equations which describe the relative motion of the undeformed surfaces of the solid spheres:

$$\frac{\mathrm{d}x}{\mathrm{d}t} = -v(t); \quad m\frac{\mathrm{d}v}{\mathrm{d}t} = -F(t), \tag{5a, b}$$

where $v(t)$ is the relative velocity of the centre of masses of the two spheres, and m is the reduced mass. We retain the inertia of the particles in our analysis, even though the inertia of the fluid is assumed negligible. This approach is valid for aerosols, since the particle density is much greater than the fluid density. For hydrosol particles, if the particle inertia is significant, then the fluid inertia is also significant during the course of their motion before the gap between them becomes small. In fact, inertia may dominate in the outer region, which yields the simple solution of nearly constant particle velocities. In most applications, however, the gap between the particles during the time in which the deformation is important is so small that our neglect of the inertia of the fluid within this narrow gap is justified. In our problem, the force $F(t)$ on the spheres is equal to the integral of the stress distribution over their surfaces. If there is also a body force present, such as a gravitational force, then this should also be included in the right-hand side of (5b). For collisions between particles having sufficient inertia to deform, an order-of-magnitude estimate reveals that the contribution to the force due to gravity is relatively small. Hence we are neglecting gravity in the present analysis. The initial conditions for (5) are $v = v_0$ and $x = x_0$ at $t = 0$.

3. Method of solution

3.1. *Asymptotic solution for small deformations*

Equations (1)–(5) are coupled and in general require numerical methods to simultaneously solve them for the dynamic deformation and pressure profiles. However, for small deformations ($w \ll x$), these equations can be solved by asymptotic methods. Let us briefly consider the leading-order solution for small deformations. By setting $w = 0$ in (1) and then solving (4) for the pressure profile, we find that

$$p(r,t) = \frac{3\mu a v}{(x + r^2/2a)^2}. \tag{6}$$

From this, the hydrodynamic force on the spheres is $F(t) = 6\pi a^2 v/x$. These results are, of course, equivalent to the well-known lubrication theory for the relative motion of rigid spheres in close contact. The presure distribution may then be used in (2) to determine the deformation profile, whence

$$w(r,t) = 12\mu\theta v\left(\frac{a}{x}\right)^{\frac{3}{2}} I\left(\frac{r}{(ax)^{\frac{1}{2}}}\right); \quad I(\xi) = \int_0^\infty \frac{\phi(\xi,\eta)}{(1+\frac{1}{2}\eta^2)^2}\,\mathrm{d}\eta. \tag{7}$$

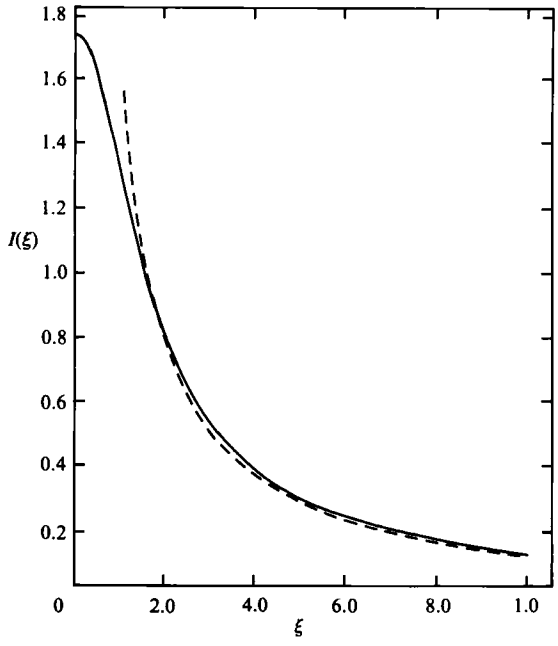

FIGURE 3. Asymptotic theory for small deformations: ——, $I(\xi)$ defined by equation (7); – – –, $\pi/2\xi$.

The integral $I(\xi)$ is plotted in figure 3, along with the asymptotic result $I \sim \pi/2\xi$ for $\xi \gg 1$, which follows from the fact that $\phi(\epsilon, \eta) \sim \pi y/2\xi$ for $\xi \gg \eta$. Also, $\phi(\xi, \eta) = \frac{1}{2}\pi$ for $\xi = 0$, so that $I(0) = \pi^2/4\sqrt{2}$, which is the maximum value of the integral.

For (6) and (7), we see that the pressure and deformation profiles depend parametrically on the values of v and x, each of which is a function of time. Dividing (5*b*) by (5*a*) in order to eliminate time, and then integrating, we find that

$$\frac{v}{v_0} = 1 - \frac{\ln(x_0/x)}{St}, \tag{8}$$

where we have used the initial conditions $v = v_0$ when $x = x_0$. Also, the Stokes number is defined as $St = mv_0/6\pi\mu a^2$ and provides a measure of the inertia of the particles relative to the viscous forces. Finally, substituting (8) into (5*a*) and solving for the separation of the undeformed surfaces as a function of time yields:

$$St\, e^{-St}\{\mathrm{Ei}(St) - \mathrm{Ei}(St - \ln(x_0/x))\} = \frac{v_0 t}{x_0}, \tag{9}$$

where Ei is the exponential integral.

The small-deformation solution described above is valid only for $w/x \ll 1$. By substituting (8) into (7), it is straightforward to show that the maximum value of w/x for $St > 0.4$ occurs at $x = x_0 \exp(0.4 - St)$ and is equal to

$$3\pi^2\epsilon \exp(2.5St - 1)/(10 > 2\ St),$$

whereas, for $St \leqslant 0.4$, the maximum value of w/x occurs at $x = x_0$ and is equal to $3\pi^2\epsilon/4\sqrt{2}$. Here, we have introduced a dimensionless elasticity parameter defined by

$$\epsilon = \frac{4\theta\mu v_0 a^{\frac{3}{2}}}{x_0^{\frac{5}{2}}}. \tag{10}$$

This parameter provides a measure of the tendency of the solids to deform. Its value must be small compared to unity in order for the deformation to be small at time $t = 0$. In aerosol and hydrosol dispersions, typical values for ϵ are in the range 10^{-7}–10^{-5} (consider, for example, 10–100 μm sandstone particles in water for which $E = 5.7 \times 10^{11}$ dyne/cm^2, $\nu = 0.10$, $\rho_s = 2.6$ g/cm^3, $\mu = 1.0$ cP, $v_0 = 10$ cm/s, and $x_0 \approx 0.01a$). A Stokes number of approximately five or greater is therefore required if the deformation is to be non-negligible. From this, we can make the rough estimate that hydrosol particles must be of radius greater than approximately 100 μm if any significant deformation is to occur during collisions, whereas solid aerosol particles as small as a few microns in size may have sufficient inertia to deform and then rebound upon impact. These estimates, of course, depend on the initial relative velocity from the outer region, as well as the physical parameters of the particles and fluid.

3.2. *Numerical analysis*

Since we are primarily interested in deformations that are sufficiently large that the spheres may rebound, the small-deformation theory described above must be supplemented by a numerical solution for larger deformations. For a given set of conditions, the small-deformation theory is used until w/x can no longer be neglected when compared with unity (in our calculations, we switched to the numerical solution when $w(0,t)/x \approx 0.05$, although the exact choice of this small number does not affect the final results). The values of x, v, and t at this point can be determined from (7)–(9). These quantities, along with the corresponding $w(r,t)$ given by (7), are then used as initial conditions for the numerical routine. The numerical computations are greatly facilitated by making the governing equations dimensionless. Using x_0 as a characteristic length in the axial direction, $(ax_0)^{\frac{1}{2}}$ as a characteristic length in the radial direction, and v_0 as a characteristic normal velocity, the only non-dimensional parameters are ϵ and St, which have been defined earlier. However, a rescaling is appropriate at the start of the numerical solution because the initial choice of x_0 is somewhat arbitrary, and x/x_0 may be much less than unity when significant deformations occur. (Recall that x_0 and v_0 are supplied by linking our solution in the inner region to the solution for the particle motion in the outer region. The only restrictions on the choice of x_0 are that $x_0/a \ll 1$, $\epsilon \ll 1$, and $Re\, x_0/a \ll 1$.) A more appropriate axial lengthscale when the deformation is significant is $x_1 = (4\theta\mu a^{\frac{3}{2}} v_0)^{\frac{2}{5}}$, which, when used in place of x_0 in (10), yields a value of unity for the scaled elasticity parameter. This rescaling greatly simplifies our analysis because only a single parameter St needs to be varied when carrying out the laborious numerical computations.

An explicit time-stepping routine, based upon finite-difference techniques, for the simultaneous numerical solution of the initial-value problem described by the dimensionless analogue of (1)–(5) suffers from instabilities such as characterize the numerical solution of parabolic differential equations. Instead, we have developed an implicit time-stepping routine, also based upon finite differences, which is quite powerful. At each new time step, a deformation profile is assumed (extrapolated from the previous time step), and the pressure distribution is computed from the numerical solution of (4). An upgraded deformation is then determined by performing the integration in (2). (We note that $\phi(r,y)$ is logarithmically singular at $y = r$. The difficulty in performing the numerical integration is overcome in the usual way by subtracting the singularity. Also, for $y/(ax_1)^{\frac{1}{2}} > 4$, the integration is performed analytically using the appropriate asymptotic expansions for the pressure profile and

for the kernel $\phi(r, y)$.) An iterative procedure is continued until the solution converges to the desired degree of accuracy. However, when the deformation becomes comparable to the undeformed gapwidth x, direct substitution of the upgraded deformation into (4) to compute an upgraded approximation for the pressure results in a diverging iteration scheme. This difficulty was also encountered by Hughes & White (1979) who computed the quasi-static deformation of two spheres subject to interparticle surface forces. The convergence of the iteration scheme has been improved by introducing an adjustable under-relaxation parameter.

As discussed earlier, the numerical computations need to be carried out only for a single value of ϵ (we chose $\epsilon = 0.01$) and varying St. The particle motion and deformation for other values of $\epsilon \ll 1$ may then be found simply by matching the numerical computations with the asymptotic solution for small deformations, and by using the fact that $x_0/x_1 \equiv \epsilon^{-\frac{2}{5}}$. The details of the numerical solution and of the transformation to other values of ϵ may be found in the thesis of Serayssol (1985).

4. Results and discussion

In order to visualize more fully the dynamic interaction between two elastic spheres, let us first examine rather comprehensive results for the single case of $(x_1/x_0)^{\frac{5}{2}} \equiv \epsilon = 0.01$ and $St = 5.0$. In figures 4–6 are plotted $h(r, t)$, $w(r, t)$, and $p(r, t)$ for these conditions. The spheres start out with a small deformation given by the asymptotic theory described previously. As the gap between the surfaces decreases, the pressure in the fluid layer increases. This pressure causes a further flattening of the particles. However, the pressure also causes the spheres to slow down, which eventually leads to a decrease in the pressure. At $\tau \equiv v_0 t/x_0 = 1.8$, the deformation of the surfaces from spherical reaches a maximum and then a relaxation occurs. Moreover, the relative velocity of the spheres is reduced to zero at $\tau = 2.1$, and the spheres then begin to rebound. As the spheres move apart, a negative pressure (relative to the bulk fluid) results as fluid is drawn in to fill the gap between the receding solid surfaces. This tensile stress opposes the motion of the spheres and limits their rebound velocity (assuming that the tensile stress does not become so large that cavitation occurs). The maximum rebound velocity is $v/v_0 = -0.34$, which occurs at $\tau = 3.0$. The fluid force prevents the spheres from escaping one another; instead, they undergo a damped oscillation and come to rest at a separation of $x/x_0 = 0.15$. This is seen more clearly in figure 7 where the force, relative velocity, and relative position of the two spheres are plotted as functions of time. Also, the kinetic energy of the two spheres, $E_k(t) = \frac{1}{2}mv^2$, and the strain energy of deformation,

$$E_s(t) = 2\pi \int_0^\infty \int_{w(r,0)}^{w(r,t)} f(r, t)\, \mathrm{d}w\, r\, \mathrm{d}r,$$

are shown in figure 8. As the spheres approach one another, rebound, and then oscillate, a portion of the kinetic energy is converted into strain energy and then restored. Eventually, however, the non-conservative viscous forces damp out this motion. The work done by the fluid is equal to the sum of the change in kinetic energy and the change in strain energy; this is also given in figure 8.

For comparison figures 9 and 10 show $h(r, t)$ for $\epsilon = 0.01$ and $St = 2.5$ and 10 respectively. When $St = 2.5$, the deformation and rebound are much less than when $St = 5.0$. On the other hand, when the inertia of the spheres is decreased to $St = 10$, there is considerable flattening of the spheres in the vicinity of contact. In fact, a very shallow dimple forms near the axis of symmetry. This can be seen more clearly

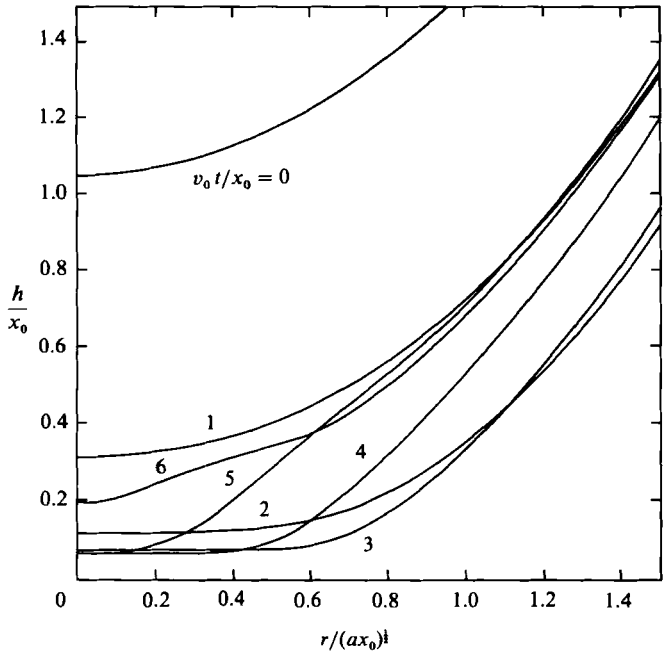

FIGURE 4. The dynamic gap profile for $St = 5$ and $\epsilon = 0.01$.

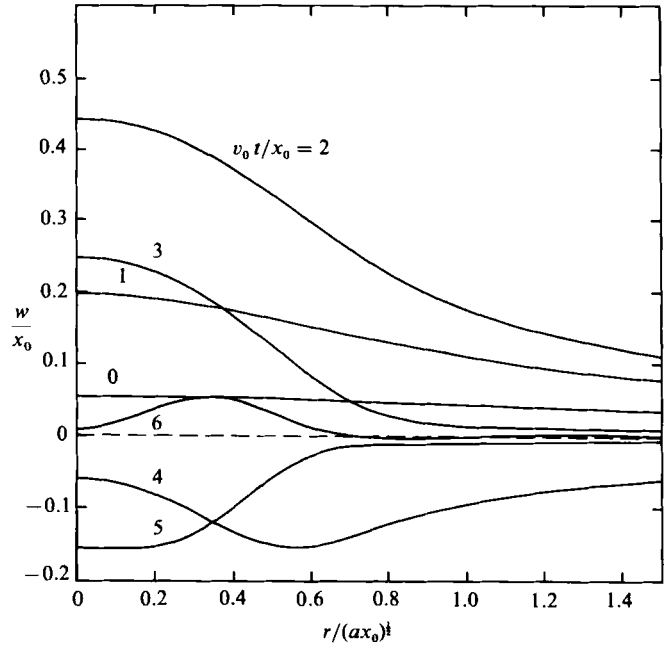

FIGURE 5. The dynamic deformation profiles for $St = 5$ and $\epsilon = 0.01$.

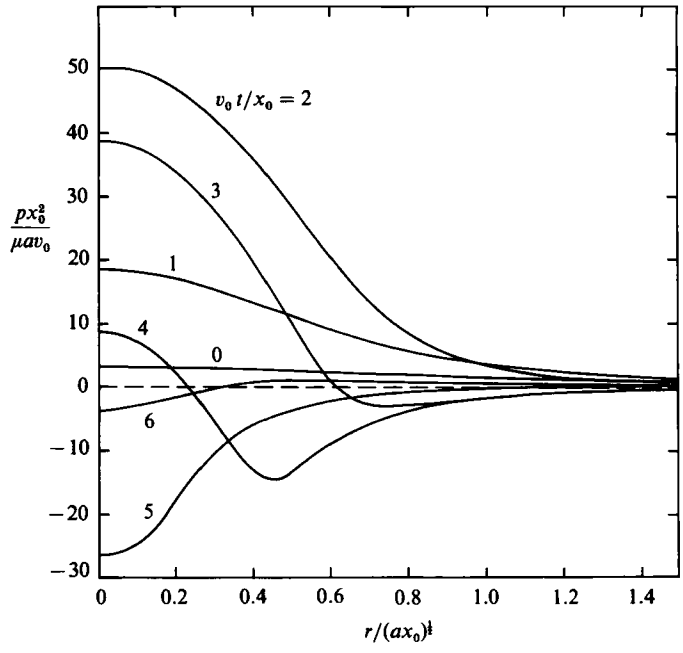

FIGURE 6. The dynamic pressure profile for $St = 5$ and $\epsilon = 0.01$.

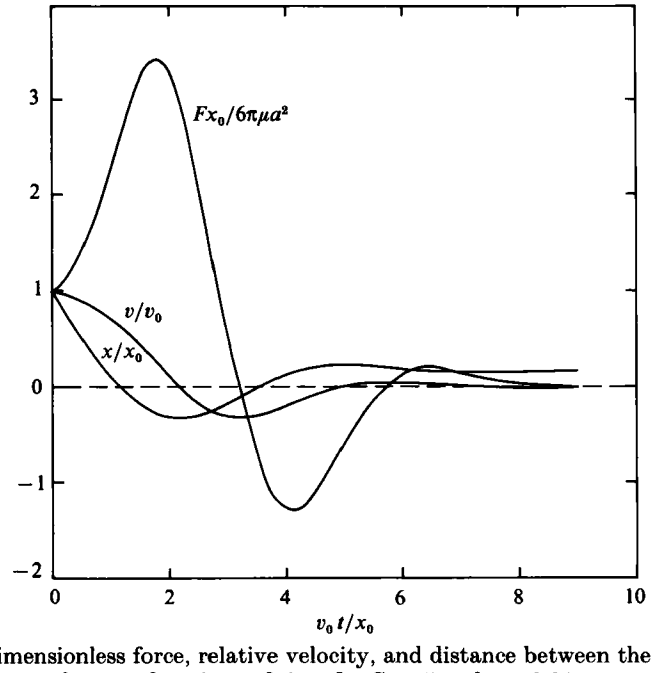

FIGURE 7. The dimensionless force, relative velocity, and distance between the undeformed surfaces as functions of time for $St = 5$ and $\epsilon = 0.01$.

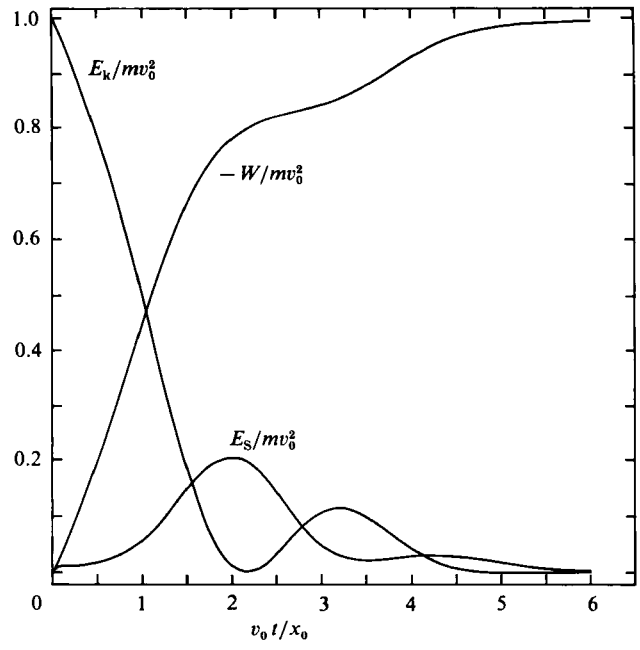

FIGURE 8. The kinetic energy (E_k), elastic strain energy of deformation (E_s), and the work done by the fluid (W) as functions of time for $St = 5$ and $\epsilon = 0.01$.

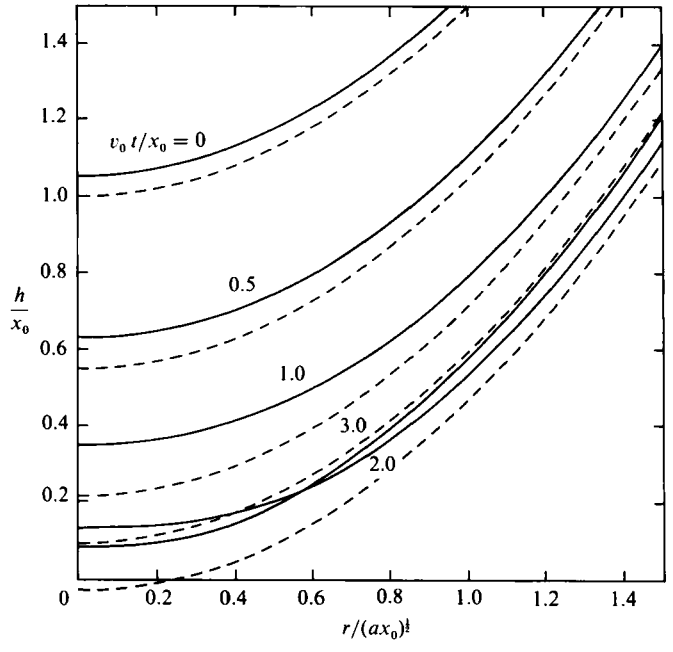

FIGURE 9. The progression with time of the undeformed and deformed gap profiles for $St = 2.5$ and $\epsilon = 0.01$: ——, the deformed-gap profile; – – –, the undeformed-gap profile.

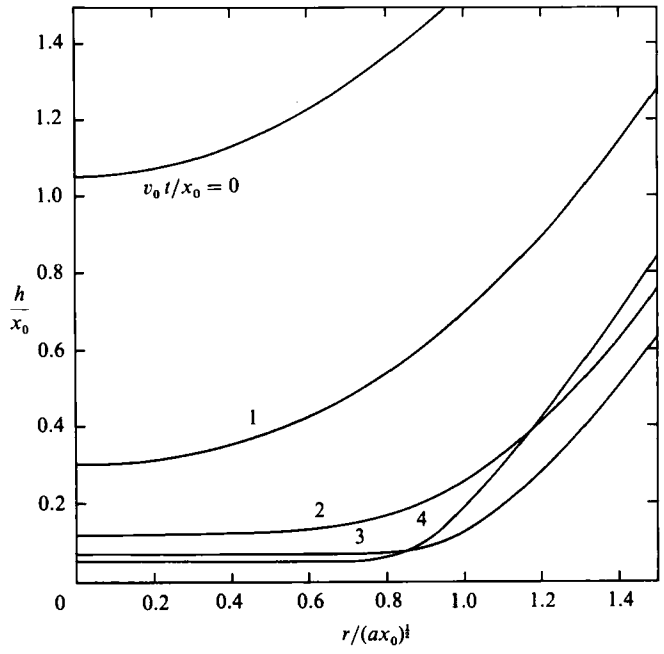

FIGURE 10. The progression with time of the deformed-gap profile with $St = 10$ and $\epsilon = 0.01$.

with the expanded scale shown in figure 11. Although dimple formation is a well-known phenomenon in the study of the motion of drops and bubbles towards surfaces (Jain & Ivanov 1980; Chen 1984), this is believed to be the first prediction of the formation of a similar dimple in a solid particle.

For figures 4–11 we chose $\epsilon = 0.01$, which is somewhat larger than typically encountered in practice, in order to focus on the region of interest, namely that where the deformation is significant. For smaller values of $\epsilon = (x_1/x_0)^{\frac{5}{2}}$, the spheres start farther apart and do not deform until x is no longer large compared to x_1. Provided that the inertia is sufficiently large ($St \gtrsim 5$) to bring the particles this close to one another, the behaviour during the final stages of approach is similar to that depicted in figures 4–11.

Of significant practical interest are the maximum rebound velocity, the closest distance of approach of the solid surfaces, and the equilibrium separation after the oscillations cease. In figures 12–14, these quantities are shown as functions of the parameters ϵ and St. As expected, the maximum rebound velocity v_r increases as both ϵ and St increase. The dimensionless rebound velocity v_r/v_0 can be thought of as a coefficient of restitution, only it measures the energy dissipated in the fluid rather than in the solid material. The closest distance of approach h_m decreases rapidly as St increases when the deformation is small (from (8) with $v = 0$), but it is relatively insensitive to St when the deformation is significant. Evidently, when the inertia of the particles is large, the very large pressure in the thin fluid layer primarily serves to flatten the particle surfaces and resists further decreases in gap size. The appropriately scaled approach distance h_m/x_1 becomes independent of ϵ when the deformation is significant ($St \gg 1$). This is expected because ϵ may be varied merely by varying the initial gap size x_0. When the particle inertia is large, the motion and resulting deformation are independent of x_0 (i.e. the decrease in the relative velocity

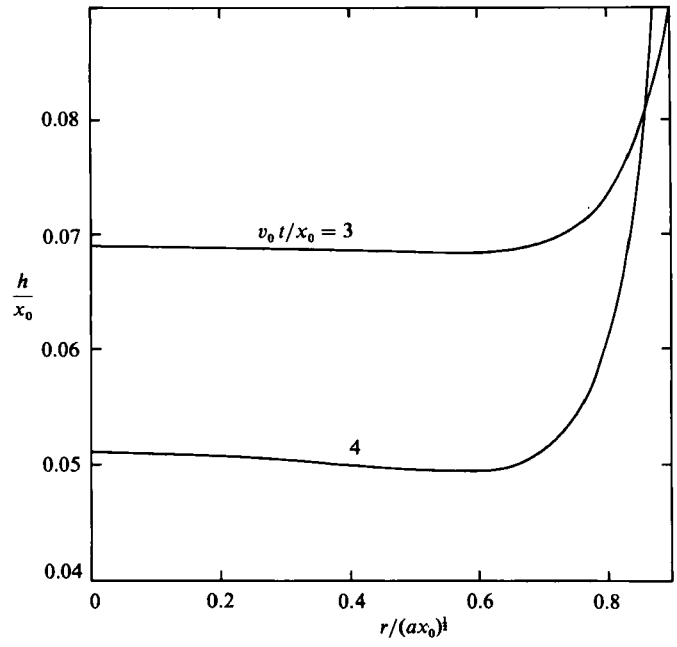

FIGURE 11. A close-up of the deformed-gap profile for $St = 10$ and $\epsilon = 0.01$.

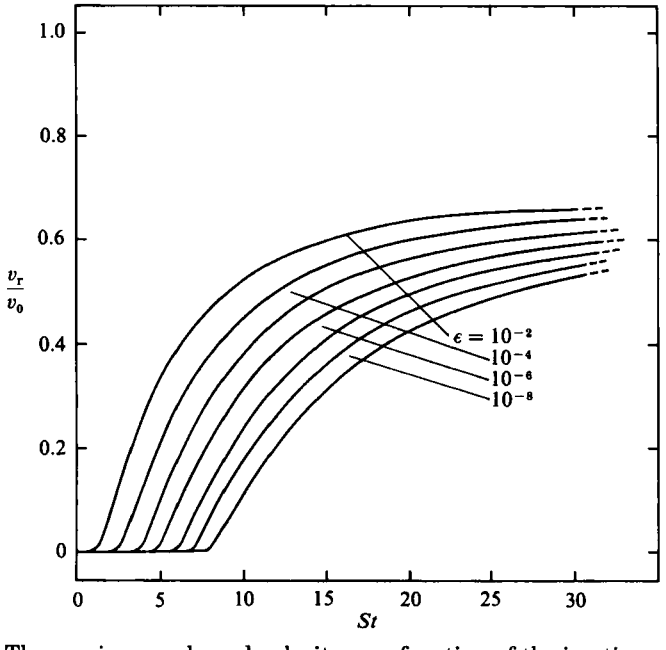

FIGURE 12. The maximum rebound velocity as a function of the inertia parameter St for various values of the elasticity parameter ϵ.

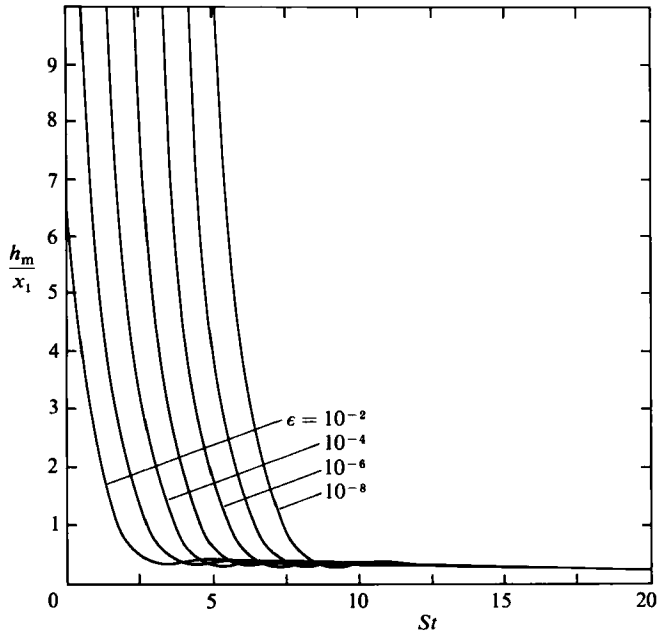

FIGURE 13. The minimum distance of approach of the deformed surfaces.

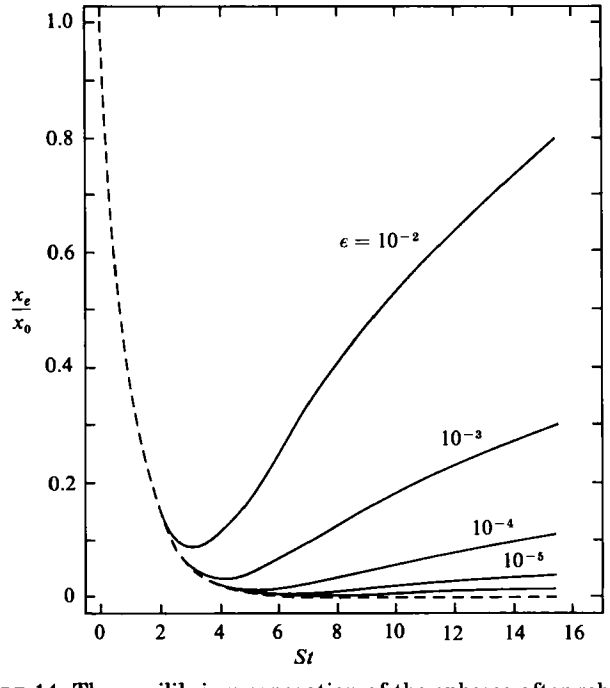

FIGURE 14. The equilibrium separation of the spheres after rebound.

of the particles as they move from one value of x_0 to a smaller value of x_0 is negligible for $St \gg 1$). Finally, in figure 14, it is seen that the equilibrium separation of the spheres x_e decreases as St increases for small St, reaches a minimum, and then increases when St is increased further. This behaviour represents a trade-off between an increased inertia, which carries the spheres closer together before they are stopped by the viscous forces, and an increased deformation, which causes the spheres to rebound further apart.

The theory and results described in this paper represent the first steps in providing rational criteria for predicting whether particles colliding in a fluid stick or rebound. Besides plasticity effects, there are several additional features which need to be taken into account in order to develop a comprehensive theory. One modification which we are currently investigating is the influence of interparticle forces of molecular origin on the motion of the particles and on the shape of their deformed surfaces (Serayssol & Davis 1985). For the non-colloidal particles considered in the present paper, i.e. particles larger than approximately one micron in size, these forces are weak unless the surfaces are very close. However, it is evident from figures 13 and 14 that the surfaces do become very close during the course of the collision, and interparticle forces may play a significant role. Moreover, for aerosol particles, the mean free path of the surrounding gas molecules is about 0.1 μm at standard conditions. Since it is very conceivable that the surfaces of the aerosol particles will approach each other more closely than this, a second need is to modify the lubrication equation of fluid dynamics (4), which is based upon the treatment of the fluid as a continuum, in order to account for the discrete molecular nature of the fluid. As shown by Hocking (1973), who used a simple Maxwell-slip model to study the relative motion of rigid spheres in aerosols, actual physical contact between the solid surfaces can occur in this case. Compressibility of the fluid may also be important during the collision of aerosol particles. For the relative motion of solid particles in liquids, it is expected that neither non-continuum nor compressibility effects will play a significant role. However, we have seen that a tensile stress (negative relative pressure) occurs as the spheres rebound. If the absolute pressure drops below the vapour pressure of the liquid, then the formation of cavitation bubbles also needs to be considered. Surface roughness may also strongly influence the collision process. For larger particles there can be significant elastic deformation in the outer region where fluid inertia is important. See Lawrence & Weinbaum (1985), Weinbaum, Lawrence & Kuang (1985) and Lawrence, Kuang & Weinbaum (1985) for a study of the role of fluid inertia in slowing down the approach of two particles. Finally, the present paper is restricted to particles in near-contact and to collisions along the line of centres. By including also the tangential component of particle collisions, one would be able to compute the trajectories of the particles in near-contact. These can then be coupled with the particle trajectories when they are not in near-contact (and when the deformation is presumably negligible) in order to determine whether the particles ultimately stick or separate.

This work was initiated while Dr Davis was an NSF-NATO post-doctoral fellow at the Department of Applied Mathematics and Theoretical Physics at the University of Cambridge. It has continued at the University of Colorado with the support of the AMOCO Foundation and of the National Science Foundation under grant CBT-844743.

Appendix

This appendix gives a Fourier transform derivation of (2) for the elastic deformation of a half-space due to an imposed axisymmetric pressure distribution. We assume that the elastic deformation is small so that linearized elasticity theory can be applied. Also if the gap is small, the particle can be approximated by a half-space, say $z > 0$. With an elastic deformation field $u(x)$, the elastic stress can be expressed, using Einstein index notation, in terms of the Lamé constants λ and μ:

$$\sigma_{ij} = \lambda\delta_{ij}u_{n,n} + \mu(u_{i,j} + u_{j,i}). \tag{A 1}$$

The conservation of momentum is

$$\sigma_{ij,j} = 0 \quad \text{in } z > 0. \tag{A 2}$$

The boundary condition of an applied normal pressure is

$$\sigma_{xz} = \sigma_{yz} = 0, \quad \sigma_{zz} = -p(x,y) \quad \text{on } z = 0. \tag{A 3}$$

We start by considering a single Fourier component in the forcing, i.e.

$$p(x,y) = \hat{p}\,\mathrm{e}^{\mathrm{i}kx}.$$

The elastic deformation then takes the form

$$\hat{u} = \mathrm{i}(c+dkz)\,\mathrm{e}^{\mathrm{i}kx-kz}, \quad \hat{v} = 0, \quad \hat{w} = (a+bkz)\,\mathrm{e}^{\mathrm{i}kx-kz}, \tag{A 4}$$

with constants a, b, c, and d to be determined. Substituting into the field equation yields

$$b+d = 0, \quad \lambda(a-b+c)+\mu(a-3b+c) = 0.$$

Substituting into the boundary conditions yields

$$a-b-c = 0, \quad \lambda k(-a+b-c)+2\mu k(-a+b) = -\hat{p}.$$

Solving, we have

$$a = \frac{\hat{p}(\lambda+2\mu)}{2k\mu(\lambda+\mu)}, \quad b = -d = \frac{\hat{p}}{2k\mu}, \quad c = \frac{\hat{p}}{2k(\lambda+\mu)}. \tag{A 5}$$

Now, the required vertical displacement of the boundary is $\hat{w}(z=0) = a$. Adding together the different Fourier components and inverting the transform of $1/k$, we find

$$w(x,y,z) = \frac{\kappa+2\mu}{4\pi\mu(\lambda+\mu)}\int\frac{p(\xi,\eta,0)}{[(x-\xi)^2+(y-\eta)^2]^{\frac{1}{2}}}\,\mathrm{d}\xi\,\mathrm{d}\eta. \tag{A 6}$$

Now, Young's elastic modulus is $E = \mu(3\lambda+2\mu)/(\lambda+\mu)$ and Poisson's ratio is $\nu = \lambda/2(\lambda+\mu)$, so that

$$(\lambda+2\mu)/\mu(\lambda+\mu) = 4(1-\nu^2)/E.$$

Finally, for an axisymmetric pressure distribution $p(r)$ we can integrate over the azimuthal angle to find the desired result:

$$w(r) = 4\frac{1-\nu^2}{\pi E}\int\frac{\rho}{r+\rho}K\left[\frac{4r\rho}{(r+\rho)^2}\right]p(\rho)\,\mathrm{d}\rho, \tag{A 7}$$

where K is the complete elliptic integral of the first kind, defined as in Abramowitz & Stegun (1964).

REFERENCES

ABRAMOWITZ, M. & STEGUN, I. A., (eds) 1964 *Handbook of Mathematical Functions.* US Govt. Printing Office, Washington.

CHEN, J.-D. 1984 Effects of London van der Waals and electric double-layer forces on the thinning of a dimpled film between a small drop or bubble and a horizontal solid plane. *J. Colloid Interface Sci.* **98**, 329.

COOLEY, M. D. A. & O'NEILL, M. E. 1969 On the slow motion generated in a viscous fluid by the approach of a sphere to a plane wall or a stationary sphere. *Mathematika* **16**, 37.

COX, R. E. & BRENNER, H. 1967 The slow motion of a sphere through a viscous fluid towards a plane surface – II. Small gap widths, including inertial effects. *Chem. Engng Sci.* **22**, 1753.

DAHNEKE, B. 1971 The capture of aerosol particles by surfaces. *J. Colloid Interface Sci.* **37**, 342.

DAHNEKE, B. 1972 The influence of flattening on the adhesion of particles. *J. Colloid Interface Sci.* **40**, 1.

DAHNEKE, B. 1973 Measurements of bouncing of small latex spheres. *J. Colloid Interface Sci.* **45**, 584.

DAVIS, R. H. 1984 The rate of coagulation of a dilute polydisperse system of sedimenting spheres. *J. Fluid Mech.* **145**, 179.

D'OTTAVIO, T. & GOREN, S. 1983 Aerosol capture in granular beds in the impaction dominated regime. *Aerosol Sci. & Tech.* **2**, 91.

ELLENBECKER, M. J., LEWITH, D. & PRICE, J. M. 1980 Impaction and particle bounce at high Stokes numbers. *J. Air Poll. Control Assoc.* **30**, 1224.

ESMEN, N. A., ZEIGLER, P. & WHITFIELD, R. 1978 The adhesion of particles upon impact. *J. Aerosol Sci.* **9**, 547.

GAL, E., TARDOS, G. & PFEFFER, R. 1985 A study of inertial effects in granular bed filtration. *AIChE J.* **31**, 1093.

GOLDSMITH, W. 1960 *Impact.* Edward Arnold.

HOCKING, L. M. 1973 The effect of slip on the motion of a sphere close to a wall and of two adjacent spheres. *J. Engng Maths* **7**, 207.

HUGHES, B. D. & WHITE, L. R. 1979 Soft contact problems in linear elasticity. *Q. J. Mech. Appl. Maths* **32**, 445.

JAIN, R. K. & IVANOV, I. B. 1980 Thinning and rupture of shaped films. *J. Chem. Soc. Faraday Trans. II* **76**, 250.

LANDAU, L. D. & LIFSHITZ, E. M. 1959 *Theory of Elasticity*, 1st English edn. Pergamon.

LAWRENCE, C. J., KUANG, Y. & WEINBAUM, S. 1985 The inertial draining of a thin fluid layer between parallel plates with a constant normal force. Part 2. Boundary layer and exact numerical solutions. *J. Fluid Mech.* **156**, 479.

LAWRENCE, C. J. & WEINBAUM, S. 1985 Hydrodynamic arrest of a flat body moving towards a parallel surface of arbitrary Reynolds number. *J. Fluid Mech.* (submitted).

LÖFFLER, F. 1980 Problems and recent advances in aerosol filtration. *Sep. Sci. Technol.* **15**, 297.

LOVE, A. E. H. 1927 *A Treatise on the Mathematical Theory of Elasticity*, 4th edn. Dover.

MELIK, D. S. & FOGLER, H. S. 1984 Gravity-induced flocculation. *J. Colloid Interface Sci.* **101**, 72.

MULLER, V. M., YUSHCHENKO, V. S. & DERJAGUIN, B. V. 1983 General theoretical consideration of the influence of surface forces on contact deformations and the reciprocal adhesion of elastic spherical particles. *J. Colloid Interface Sci.* **92**, 92.

PAYATAKES, A. C. & GRADON, L. 1980 Dendritic deposition of aerosol particles in fibrous media by inertial impaction and interception. *Chem. Engng Sci.* **35**, 1083.

PRODI, F. & TAMPIERI, F. 1982 The removal of particulate matter from the atmosphere: the physical mechanisms. *PAGEOPH* **120**, 286.

PRUPPACHER, H. R. & KLETT, J. D. 1978 *Microphysics of Clouds and Precipitation.* Reidel.

SCHOWALTER, W. R. 1984 Stability and coagulation of colloids in shear fields. *Ann. Rev. Fluid Mech.* **16**, 245.

SERAYSSOL, J.-M. 1985 Dynamic deformation and rebound of particles during filtration and coagulation. M.S. thesis, University of Colorado, Boulder, Colorado.

SERAYSSOL, J.-M. & DAVIS, R. H. 1985 The influence of surface interactions on the elastohydrodynamic collision of two spheres. *J. Colloid Interface Sci.* (submitted).

TARDOS, G. I., YU, E., PFEFFER, R. & SQUIRES, A. M. 1979 Experiments on aerosol filtration in granular sand beds. *J. Colloid Interface Sci.* **71**, 616.

TIEN, C. & PAYATAKES, A. C. 1979 Advances in deep bed filtration. *AIChE J.* **25**, 737.

TSIANG, R. C., WANG, C.-S. & TIEN, C. 1982 Dynamics of particle deposition in model filter fibers. *Chem. Engng Sci.* **37**, 1661.

WEINBAUM, S., LAWRENCE, C. J. & KUANG, Y. 1985 The inertial draining of a thin fluid layer between parallel plates with a constant normal force. Part 1. Analytic solutions; inviscid and small- but finite-Reynolds-number limits. *J. Fluid Mech.* **156**, 463.